**Blagoja MARKOVSKI[1], Leonid GRCEV[2], Vesna ARNAUTOVSKI-TOSEVA[1],
Jasmina ANGELEVSKA KOSTADINOVSKA[1], Andrijana KUHAR[1]**

Ss Cyril and Methodius University in Skopje (1), Macedonian Academy of Sciences and Arts (2)

Improving Efficiency of Full-Wave Electromagnetic Analysis of Grounding Systems Within Homogeneous Earth

Abstract. Efficient approach for full-wave modelling of grounding systems is provided. First the electric field integral equations are cast in form that is more suitable for grounding analysis and have improved convergence. Then numerical evaluation of the Sommerfeld integrals is substituted by bivariate cubic interpolation procedure of the solutions from pre-computed interpolation grid. This procedure provides substantial improvement of efficiency of the full-wave electromagnetic analysis of grounding systems, while introducing a negligible error in the results.

*Streszczenie. W artykule opisano efektywne podejście do modelowania systemów uziemiających. W pierwszej części podano równania różniczkowe opisujące pole elektryczne w formie, która jest bardziej odpowiednia dla analizy uziemienia i pozwala na uzyskanie lepszej zbieżności z wynikami eksperymentu. Następnie obliczenia numeryczne całek Sommerfelda zastąpiono dwuzmienną interpolacją sześcienną rozwiązań z wcześniej obliczonej siatki interpolacyjnej. Ta procedura zapewnia znaczną poprawę wydajności pełnej elektromagnetycznej analizy układów uziemienia, jednocześnie wprowadzając nieznaczny błąd w wynikach. (**Poprawa efektywności analizy elektromagnetycznej układów uziemienia w jednorodnym środowisku ziemi**).*

Keywords: grounding systems, Sommerfeld integral, analysis of grounding systems
Słowa kluczowe: układy uziemienia, całka Sommerfelda, analiza układów uziemienia

Introduction

The frequency dependent and transient characteristics of grounding systems are of interest in many engineering analyses related to electric power safety and lightning protection, where frequencies of interest range from dc to few MHz [1], and electromagnetic compatibility related studies, with frequencies of interest up to tens of MHz [2]. Different methods for modelling of grounding systems have been developed in the past few decades, based on electric circuit [3, 4], transmission line [5] and electromagnetic theory [6]. Among them, electromagnetic model provides most accurate results for all frequencies of interest.

The most popular electromagnetic model is based on antenna theory and solution of electric field integral equations by the method of moments (MoM) [6, 7]. One difficulty in implementation of the mathematically exact solution for the electric field for semi-infinite conducting medium in practical problems is the numerical evaluation of singular, oscillatory and slow converging Sommerfeld integrals, which is numerically unstable and extremely time consuming procedure. To circumvent this problem in practical analysis, quasi-static [8, 9] or complex-images approximations [10, 11] are often employed, however, the governing approximations limit their validity to a certain upper frequency and system dimensions. Due to the lack of efficient full-wave model, the domain of applicability of these approximations as well as other approximate models has not been rigorously tested for wide range of parameters and complex configurations.

Another common problem in the application of antenna theory based methods for analysis of buried conductors is that they may not provide exact solutions for low frequencies approaching 0 Hz. This is either due to improper treatment of the images of currents in conductors [9], or due to numerical instabilities often referred to as "low frequency breakdown".

This paper presents efficient approach for full-wave modelling of grounding systems with arbitrary shape. First the electric field integral equations are cast in form that is more suitable for grounding analysis, since it provides exact solutions from 0 Hz to frequencies in the MHz range and improved convergence and behaviour of the Sommerfeld integrals. Then numerical evaluation of the new form of Sommerfeld integrals is substituted by bivariate cubic interpolation procedure of the solutions from the pre-computed interpolation grid. This procedure provides substantial improvement of efficiency of the full-wave electromagnetic analysis of grounding systems, while introducing a negligible error in the results that may also serve as reference for extensive comparison of approximate models. Accuracy and efficiency of the presented approach are validated by results comparison with full-wave model that utilizes direct numerical integration.

General description of the mathematical model

Grounding system is considered as network of connected straight wires with arbitrary orientation, below the earth surface. Each wire is divided in N short cylindrical segments, for which the so called thin-wire approximation is applied. By this approximation, conductor volumes are reduced to short and thin filaments. This allows both longitudinal currents and charges to be represented by line distributions along the cylinder axis. Solution of the problem is based on MoM, using pulse basis functions for the current and point matching for testing boundary conditions regarding the tangential component of the electric field at the wire surface [7]. Current distribution on the structure, for any type of excitation [12] is found by solving the matrix equation:

$$(1) \qquad [Z][I] = [V]$$

where $[Z]$ is generalized impedance matrix, $[I]$ is vector of unknown currents and $[V]$ is vector of excitations. Elements z_{mn} of the generalized impedance matrix represent the self or mutual impedances between pairs of test and source segments. They can be expressed in terms of the tangential component of the electric field vector $\vec{E}_n$ at the surface of the test segment m, due to longitudinal current I_n in the source segment n [7].

Integral equations of the electric field can be formulated in various ways. Amongst, the mixed-potentials integral equation (MPIE) [13] formulation is preferable for grounding analysis since it provides some advantages over other possible variants [14]: Sommerfeld integrals converge faster and spatial Green functions are less singular than their derivatives in other variants e.g. [15]; provides separate

treatment of the contributions from longitudinal and leakage currents; with proper adjustment MPIE enables exact application of image theory at 0 Hz.

In MPIE formulation, the scattered electric field vector $\vec{E}^s(\vec{r})$ is expressed in terms of magnetic vector potential $\vec{A}(\vec{r})$ and electric scalar potential $\Phi(\vec{r})$, due to longitudinal current $I(\vec{r}')$ along the axis of the source segment ℓ'.

$$(2) \qquad \vec{E}^s(r) = -j\omega\vec{A}(r) + \nabla\Phi(r)$$

$$(3) \qquad \vec{A}(\vec{r}) = \int_{\ell'} \overline{\overline{G}}_A(\vec{r},\vec{r}') I_n(\vec{r}') d\vec{\ell}'$$

$$(4) \qquad \Phi(\vec{r}) = \int_{\ell'} G_\Phi(\vec{r},\vec{r}') \nabla' I(\vec{r}') d\ell'$$

Here, $\overline{\overline{G}}_A$ is a dyadic Green's function of the magnetic vector potential and G_Φ is a Green's function of the electric scalar potential. Green's functions are actually potentials at point $\vec{r}(x,y,z)$ produced by unit-strength arbitrarily oriented current dipole at point $\vec{r}'(x',y',z')$.

Spatial domain Green's functions in formulation B

Different formulations of Green's functions for magnetic vector potentials are available [16]. Here we adopt formulation B for source and evaluation points in semi-infinite conducting medium characterized by conductivity σ_1, permeability μ_0 and permittivity ε_1, as illustrated on Fig. 1.
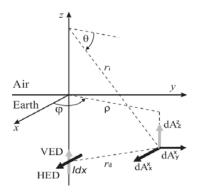

Fig.1. Magnetic vector potential components for HED and VED

The dyadic Green's function for magnetic vector potential due to electric dipole with arbitrary orientation can be expressed by the contributions of electric dipoles with two typical positions, x-oriented horizontal electric dipole (HED) and z-oriented vertical electric dipole (VED):

$$(5) \qquad \overline{\overline{G}}_A = \hat{x}\hat{x}' G_A^{xx} + \hat{y}\hat{y}' G_A^{yy} + (\hat{x}\hat{y}' + \hat{y}\hat{x}') G_A^{xy} + \hat{z}\hat{z}' G_A^{zz}$$

where $\hat{x}'$, $\hat{y}'$ and $\hat{z}'$ are direction cosines of source dipole, and $\hat{x}$, $\hat{y}$ and $\hat{z}$ are direction cosines of calculated magnetic vector potential in local coordinate system shown in Fig. 1.

The Green's function for the scalar potential follows from the application of the Lorentz gauge, for example:

$$(6) \qquad \frac{\partial}{\partial z'} G_\Phi = -\frac{j\omega}{\mu_0\underline{\sigma}_1} G_A^{zz}$$

Spatial domain Green's functions, for horizontal and vertical electrical dipole in semi-infinite conducting media, can be presented in various forms. The most general is written as a sum of the contribution from direct term and the influence of the air-earth interface in integral form:

$$(7) \qquad G_A^{xx} = \frac{\mu_0}{4\pi}\left[\frac{e^{-jk_1 r_d}}{r_d} + \frac{1}{2}(I_1' + \cos(2\varphi)I_2')\right]$$

$$(8) \qquad G_A^{yy} = \frac{\mu_0}{4\pi}\left[\frac{e^{-jk_1 r_d}}{r_d} + \frac{1}{2}(I_1' - \cos(2\varphi)I_2')\right]$$

$$(9) \qquad G_A^{xy} = \frac{\mu_0}{4\pi}\left[\frac{1}{2}\sin(2\varphi)I_2'\right]$$

$$(10) \qquad G_A^{zz} = \frac{\mu_0}{4\pi}\left[\frac{e^{-jk_1 r_d}}{r_d} + I_3'\right]$$

$$(11) \qquad G_\Phi = \frac{1}{4\pi\underline{\sigma}_1}\left[\frac{e^{-jk_1 r_d}}{r_d} - I_3'\right]$$

$$(12) \qquad I_1' = \int_0^\infty \left(R_{10}^{TE} - R_{10}^{TM}\right)\frac{e^{-jk_{z1}|z+z'|}}{jk_{z1}} J_0(k_\rho\rho)k_\rho\,dk_\rho$$

$$(13) \qquad I_2' = \int_0^\infty \left(R_{10}^{TE} + R_{10}^{TM}\right)\frac{e^{-jk_{z1}|z+z'|}}{jk_{z1}} J_2(k_\rho\rho)k_\rho\,dk_\rho$$

$$(14) \qquad I_3' = \int_0^\infty R_{10}^{TM}\frac{e^{-jk_{z1}|z+z'|}}{jk_{z1}} J_0(k_\rho\rho)k_\rho\,dk_\rho$$

To avoid numerical instability at low frequencies approaching to 0 Hz, all frequency dependent parameters in (7)-(14) are expressed in terms of the complex conductivity $\underline{\sigma}_n$ of n-th region (n=0 for the air, and n=1 for the earth):

$$\underline{\sigma}_n = \sigma_n + j\omega\varepsilon_n, \quad k_n = \sqrt{-j\omega\mu_n\underline{\sigma}_n}, \quad k_{zn} = \sqrt{k_n^2 - k_\rho^2}$$

$$R_{10} = \frac{\underline{\sigma}_1 - \underline{\sigma}_0}{\underline{\sigma}_1 + \underline{\sigma}_0}, \quad R_{10}^{TE} = \frac{jk_{z1} - jk_{z0}}{jk_{z1} + jk_{z0}}, \quad R_{10}^{TM} = \frac{\underline{\sigma}_0 k_{z1} - \underline{\sigma}_1 k_{z0}}{\underline{\sigma}_0 k_{z1} - \underline{\sigma}_1 k_{z0}}$$

Here, R_{10}^{TE}, R_{10}^{TM} and R_{10} are Fresnel TE, TM and quasi-static reflection coefficients, k_{zn} and k_n are vertical wave number and propagation constant for the corresponding n-th region, and k_ρ is radial wave number. The geometric quantities $\rho=[(x-x')^2+(y-y')^2]^{-2}$ and $\Delta z_p=|z+z'|$ are the radial and vertical distance between the source image and evaluation point, respectively.

Analysis of characteristics of the Sommerfeld integrals

For a fixed set of frequency and earth characteristics, when source and observation points are located in same semi-infinite region, the integral equations in the Green's functions depend on the two geometric quantities ρ and Δz_p. This allows for named integral equations to be pre-computed for a discrete set of values for ρ and Δz_p in a two-dimensional interpolation grid, and then, the required solutions of integral parts in Green's functions can be readily obtained by suitable interpolation method.

Interpolation of the Sommerfeld integrals is commonly used method for improving the efficiency in antenna analysis [17, 18]. This approach is already implemented for improving the efficiency of the well known antenna code NEC [19] and electromagnetic simulation software FEKO, but for a different set of integral equations optimized for antenna analysis. Here, similar procedure in improving the efficiency is applied, for evaluation of the set of integral equations (12)-(14). In the following analysis the interpolation grid will be generated for another two geometric parameters, related to ρ and Δz_p: the distance between the source image location and evaluation point, $r_i=(\rho^2+\Delta z_p^2)^{-2}$, and the angle between vectors, $\theta=\tan^{-1}(\rho/\Delta z_p)$, illustrated on Fig. 1. For a fixed set of parameters f= 10 MHz, σ_1 = 0.01 S/m, ε_1 = 10ε_0 and $\mu_1 = \mu_0$, using the numerical integration procedure

provided in [20], the following interpolation surfaces and convergence characteristics are obtained, as illustrated in Fig. 2.

The solutions of Sommerfeld integrals (12)-(14), illustrated on Fig. 2, show singular behaviour and numerical instability for $r_i/\lambda_1 \to 0$, and slow convergence (up to $2 \cdot 10^6$

calls of integrand) for $\theta \to 0$. These conditions are met for source and evaluation points at great distance near the earth surface, which is especially unfortunate for analysis of large grounding systems. Due to the steep variations of solutions, obtained surfaces are not suitable for interpolation.
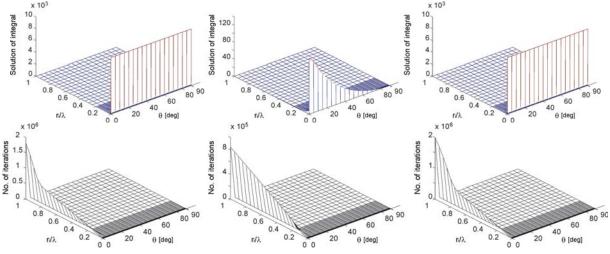

Fig.2. Solutions (upper) and number of iterations to convergence (lower figures) for integrals I'_1, I'_2 and I'_3 before singularities extraction

Development of new form of Green's functions

To increase convergence of the Sommerfeld integrals and obtain smooth variations in the spatial domain, singularities from integrals (12)-(14) will be extracted in form of their low frequency approximations [21]. For low frequencies approaching to 0 Hz, the approximation $k_{z0} \approx k_{z1} \approx k_\rho$ is valid, so the following approximation for the reflection coefficients is obtained:

$$(15) \qquad R_{10}^{TE} \cong 0, \quad R_{10}^{TM} \cong -R_{10}$$

By substitution of reflection coefficients (15) in (12)-(14), extraction of the derived low frequency approximations of integrals (12)-(14) and considering the following identities:

$$(16) \qquad \int_0^\infty \frac{e^{-jk_{z1}|z+z'|}}{jk_{z1}} J_0(k_\rho \rho) k_\rho \, dk_\rho = \frac{e^{-jk_1 r_i}}{r_i}$$

$$(17) \qquad \int_0^\infty \frac{e^{-jk_{z1}|z+z'|}}{jk_{z1}} J_2(k_\rho \rho) k_\rho \, dk_\rho = \frac{2\left(e^{-jk_1|z+z'|} - e^{-jk_1 r_i}\right)}{jk\rho^2} - \frac{e^{-jk_1 r_i}}{r_i}$$

new form of Green functions (7)-(11) is derived:

$$(18)$$
$$G_A^{xx} = \frac{\mu_0}{4\pi} \left[\begin{array}{l} \dfrac{e^{-jk_1 r_d}}{r_d} + R_{10} \dfrac{e^{-jk_1 r_i}}{2r_i} + \dfrac{1}{2}(I_1 + \cos(2\varphi)I_2) \\[2ex] -R_{10}\cos(2\varphi)\left(\dfrac{e^{-jk_1|z+z'|} - e^{-jk_1 r_i}}{jk\rho^2} - \dfrac{e^{-jk_1 r_i}}{2r_i} \right) \end{array} \right]$$

$$(19)$$
$$G_A^{yy} = \frac{\mu_0}{4\pi} \left[\begin{array}{l} \dfrac{e^{-jk_1 r_d}}{r_d} + R_{10} \dfrac{e^{-jk_1 r_i}}{2r_i} + \dfrac{1}{2}(I_1 - \cos(2\varphi)I_2) \\[2ex] +R_{10}\cos(2\varphi)\left(\dfrac{e^{-jk_1|z+z'|} - e^{-jk_1 r_i}}{jk\rho^2} - \dfrac{e^{-jk_1 r_i}}{2r_i} \right) \end{array} \right]$$

$$(20)$$
$$G_A^{xy} = -\frac{\mu_0}{4\pi} \left[\begin{array}{l} R_{10} \sin(2\varphi)\left(\dfrac{e^{-jk_1|z+z'|} - e^{-jk_1 r_i}}{jk\rho^2} - \dfrac{e^{-jk_1 r_i}}{2r_i} \right) \\[2ex] -\dfrac{1}{2}\sin(2\varphi)I_2 \end{array} \right]$$

$$(21) \qquad G_A^{zz} = \frac{\mu_0}{4\pi} \left[\frac{e^{-jk_1 r_d}}{r_d} - R_{10}\frac{e^{-jk_1 r_i}}{r_i} + I_3 \right]$$

$$(22) \qquad G_\Phi = \frac{1}{4\pi\underline{\sigma}_1} \left[\frac{e^{-jk_1 r_d}}{r_d} + R_{10}\frac{e^{-jk_1 r_i}}{r_i} - I_3 \right]$$

$$(23) \qquad I_1 = \int_0^\infty \left(R_{10}^{TE} - R_{10}^{TM} - R_{10} \right) \frac{e^{-jk_{z1}|z+z'|}}{jk_{z1}} J_0(k_\rho\rho) k_\rho \, dk_\rho$$

$$(24) \qquad I_2 = \int_0^\infty \left(R_{10}^{TE} + R_{10}^{TM} + R_{10} \right) \frac{e^{-jk_{z1}|z+z'|}}{jk_{z1}} J_2(k_\rho\rho) k_\rho \, dk_\rho$$

$$(25) \qquad I_3 = \int_0^\infty \left(R_{10}^{TM} + R_{10} \right) \frac{e^{-jk_{z1}|z+z'|}}{jk_{z1}} J_0(k_\rho\rho) k_\rho \, dk_\rho$$

It is important to note that terms related to I_1, I_2 and I_3 in equations (18)-(22) are the difference between the application of the low frequency approximation of Green's functions for formulation B and the full-wave electromagnetic theory formulated by MPIE. For frequencies approaching 0 Hz the solution of these integrals approaches to 0, and therefore, (18)-(22) provides exact solution for all frequencies of interest, starting from 0 Hz.

In Fig. 3, surfaces for integrals (23)-(25) are illustrated for the same set of parameters as used in the previous analysis. Results show that extraction of the singularities significantly increases the efficiency of numerical evaluation of Green's functions. Integrals do not show singular behaviour and instability, while the convergence is substantially improved. More important, the interpolation surfaces are significantly smoothed, which permits use of sparse interpolation grids.
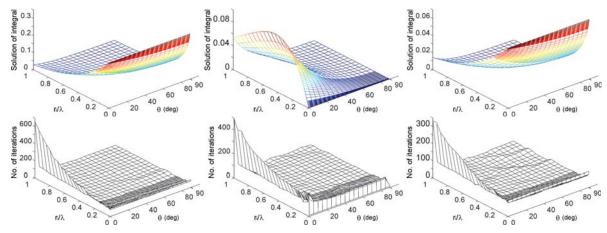
Fig.3. Solutions (upper) and number of iterations to convergence (lower figures) for integrals I_1, I_2 and I_3 before singularities extraction

Reduced number of points in the interpolation grids, together with the improved convergence, provides substantial reduction of computation times in generating interpolation grids, which is especially important for time-domain analysis in transient and lightning related studies where high number of frequencies are involved.

Validation of efficiency and accuracy of the presented approach

The presented approach is validated by two examples, illustrated on Fig. 4:

1) horizontal grounding grid with 50 x 100 m side lengths, composed of square meshes with conductor spacing equal to 5 m, buried at depth of 0.5 m. Such grounding grid is typically subject of electric power safety analysis. Due to the large system dimensions, interpolation grid for distances up to $r_{i\,max}=10\lambda_1$ will be required for soil with good conductivity, and frequencies up to 10 MHz.

2) grounding system with arbitrarily oriented electrodes, that occupies a volume of 15 x 15 x 3 m. Such grounding system is typical for wind turbines.

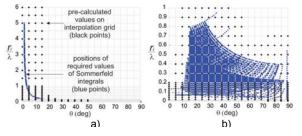Fig.4. Analyzed geometries: a) horizontal grounding grid, b) wind turbine grounding system.

Fig.5. Positions of required (blue) and pre-computed (black) elements in interpolation grids for: a) horizontal grounding grid, b) wind turbine grounding system.

In both cases, perfect electric conductors with 7-mm radius are considered, buried in uniform soil with resistivity ρ_1 equal to 30, 300 and 3000 Ωm, with permeability $\mu_1 = \mu_0$ and permittivity $\varepsilon_1 = 10\varepsilon_0$. Currents with frequencies from 10 Hz to 10 MHz, are injected in the centre of the grounding systems.
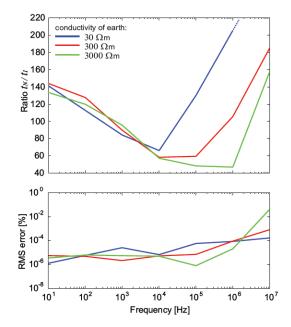

Fig.5. Validation of efficiency (upper) and accuracy of analysis (lower figure) for horizontal grounding grid
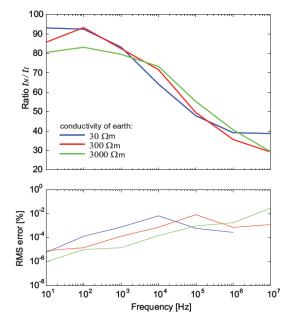

Fig.6. Validation of efficiency (upper) and accuracy of analysis (lower figure) for wind turbine grounding system

The structures in both cases are divided to around $N \approx 1200$ segments. Variable size interpolation grid is generated, relative to the analyzed frequency and soil characteristics. The elements of the interpolation grid are not pre-computed, but they are computed and stored as required. Solutions for integrals (23)-(25) in Green's functions (18)–(22) are then obtained by bivariate interpolation. The positions of required and pre-computed elements in interpolation grid, for the analyzed cases, for a frequency of 1 MHz and earth resistivity ρ_1=300 Ωm are illustrated on Fig. 5.

For a given set of parameters for both cases, efficiency and accuracy of the proposed method are validated by comparison of:
- ratio of evaluation times for currents distribution on structures in both cases, obtained by numerical integration (t_N) and with interpolation of the Sommerfeld integrals (t_I) in equations (23)-(25);
- the RMS error for longitudinal currents in electrodes of grounding systems, evaluated as [22]:

$$(26) \qquad \varepsilon_{RMS} = \left[\frac{\sum_{n=1}^{N} \left| I_n^{INT} - I_n^{NUM} \right|^2}{\sum_{n=1}^{N} \left| I_n^{NUM} \right|^2} \right]^{1/2} \times 100(\%)$$

where I_n^{INT} and I_n^{NUM} are computed complex coefficients of current at N segments, obtained by interpolation and numerical evaluation of Sommerfeld integrals.

Conclusions

With the presented adjustments of the MPIE formulated integral equations and the implemented interpolation method, following benefits are achieved:
- electric field integral equations are cast in form that provides exact solution for all frequencies of interest, starting from 0 Hz to frequencies in the MHz range;
- substantial improvement of convergence is obtained by extraction of singularities from the integral equations;
- interpolation surfaces are smoother, and therefore, sparse interpolation grids with less elements are required;
- the presented procedure provides substantial reduction of computation times, from 30 to 200 times depending on the analyzed case, as illustrated on Fig. 6 and Fig. 7;
- the interpolation procedure provides nearly exact results, introducing errors smaller that 0.1% for longitudinal currents distribution in electrodes, as illustrated on Fig. 6 and Fig. 7;

- considering minor introduced errors, this procedure may serve as reference for scientific and practical applications.

Authors: *msc Blagoja Markovski, prof. dr Vesna Arnautovski-Toseva, msc Jasmina Angelevska Kostadinivska and ass. prof. dr Andrijana Kuhar are with the Ss Cyril and Methodius University in Skopje, Faculty of Electrical Engineering and Information Technologies, Rugjer Boskovic 18, P.O. box 574, Skopje, Macedonia, E-mail: bmarkovski@feit.ukim.edu.mk; atvesna@feit.ukim.edu.mk; jasminaa@feit.ukim.edu.mk; kuhar@feit.ukim.edu.mk; prof. dr Leonid Grcev is with the Macedonian Academy of Sciences and Arts, Skopje 1000, Macedonia E-mail: lgrcev@feit.ukim.edu.mk.*

REFERENCES
[1] Grcev L., Modeling of grounding electrodes under lightning current, *IEEE Trans. Electromagn. Compat.*, 51 (2009), No. 3, 559-571.
[2] Grcev L., Deursen A.P.J. and Waes J.B.M., Lightning current distribution to ground at a power line tower carrying a radio base station, *IEEE Trans. Electromagn. Compat.*, 47 (2005), No. 1, 160-170.
[3] Otero A.F., Cidras J. and Alamo J.L., Frequency-dependent grounding grid calculation by means of a conventional nodal analysis technology, *IEEE Trans. Power Del.*, 14 (1999), No. 3, 873–877.
[4] Yutthagowith P., Ametani A., Nagaoka N. and Baba Y., Application of the partial element equivalent circuit method to analysis of transient potential rises in grounding systems. *IEEE Trans. Electromagn. Compat.*, 53 (2011), No. 3, 726–736.
[5] Sunde E. D., *Earth conduction effects in transmission systems*, 2nd ed., (1968), New York: Dover.
[6] Grcev L. and Dawalibi F., An electromagnetic model for transients in grounding systems, *IEEE Trans. Power Del.*, 5 (1990), No. 2, 1773–1781.
[7] Harrington R. F., Matrix methods for field problems, *Proc. of IEEE*, 55 (1967), No. 2, 136-149.
[8] Grcev L. and Grceva S., Comparison between exact and quasi-static methods for HF analysis of horizontal buried wires, *IEEE Trans. Electromagn. Compat.*, 51 (2009), No. 4, 1051-1054.
[9] Arnautovski-Toseva V. and Grcev L., On the image model of a buried horizontal wire, *IEEE Trans. Electromagn. Compat.*, 58 (2016), No. 1, 278-286.
[10] Bannister P., Applications of complex image theory, *Radio Science*, 21 (1986), No. 4, 605-616.
[11] Chow Y.L., Yang J.J. and Srivastava K.D., Complex images of a ground electrode in layered soils, *Journal of Applied Physics*, 71 (1992), No. 2, 569-574.
[12] Grcev L., Rachidi F. and Rakov V.A., Comparison of electromagnetic models of lightning return strokes using current and voltage sources. *Paper presented at 12th International Conference on Atmospheric Electricity, ICAE'03*, (2003) Versailles, France.
[13] Michalski K.A., The mixed-potential electric field integral equation for objects in layered media. *Archiv fur Elektronik und Übertragungstechnik*, 39 (1985), 317-322.
[14] Vandenbosch G.A.E. and Capelle A.R., Mixed-potential integral expression formulation of the electric field in a stratified dielectric medium-application to the case of a probe current source. *IEEE Trans. Antennas Propagat.*, 40 (1992), No. 7, 806-817.
[15] Banos A., *Dipole radiation in the presence of a conducting half-Space*, (1966), Oxford: Pergamon Press.
[16] Michalski K.A. and Zheng D., Electromagnetic scattering and radiation by surfaces of arbitrary shape in layered media, Part I: Theory. *IEEE Trans. Antennas Propagat.*, 38 (1990), No. 3, 335-344.
[17] Burke G.J. and Miller E.K., Modeling antennas near to and penetrating a lossy interface. *IEEE Trans. Antennas Propagat.*, 32 (1984), No. 10, 1040–1049.
[18] Brittingham J.N., Miller E.K. and Okada J.T., A bivariate interpolation approach of efficiently and accurately modeling of antennas near a half space. *Electronics Letters*, 13 (1977), No. 23, 690–691.
[19] Burke G.J., Numerical Electromagnetic Code – NEC4, *UCRL-MA-109338.*, (1992).
[20] Lytle R.J. and Lager D.L., Numerical evaluation of Sommerfeld integrals, *UCRL-51688*, (1974), Lawrence Livermore National Laboratory, CA.
[21] Bunger R. and Arndt F., Efficient MPIE approach for the analysis of threedimensional microstrip structures in layered media, *IEEE Trans. on Microwave Theory and Techniques*, 45 (1997), No. 8, 1141–1153.
[22] Poggio A., Bevensee R. and Miller E.K., Evaluation of some thin wire computer programs. *IEEE Antennas Propag. Symp.*, 12 (1974), 181–184.